ACS chemical biology

Articles

pubs.acs.org/acschemicalbiology

N-Methylation as a Strategy for Enhancing the Affinity and Selectivity of RNA-binding Peptides: Application to the HIV-1 Frameshift-Stimulating RNA

Thomas A. Hilimire,[†] Ryan P. Bennett,[§] Ryan A. Stewart,[§] Pablo Garcia-Miranda,[∥] Alex Blume,[∥] Jordan Becker,[⊥] Nathan Sherer,[⊥] Eric D. Helms,[#] Samuel E. Butcher,[∥] Harold C. Smith,[†,§] and Benjamin L. Miller*[,†,‡]

[†]Departments of Biochemistry and Biophysics, and [‡]Dermatology, University of Rochester, Rochester, New York 14642, United States

[§]OyaGen, Inc., Rochester, New York 14623, United States

[∥]Department of Biochemistry, University of Wisconsin, Madison, Wisconsin 53706, United States

[⊥]McArdle Laboratory for Cancer Research and Institute for Molecular Virology, University of Wisconsin-Madison, Madison, Wisconsin 53706, United States

[#]Department of Chemistry, SUNY Geneseo, Geneseo, New York 14454, United States

Supporting Information

ABSTRACT: Human Immunodeficiency Virus (HIV) type 1 uses a −1 programmed ribosomal frameshift (−1 PRF) event to translate its enzymes from the same transcript used to encode the virus' structural proteins. The frequency of this event is highly regulated, and significant deviation from the normal 5−10% frequency has been demonstrated to decrease viral infectivity. Frameshifting is primarily regulated by the Frameshift Stimulatory Signal RNA (FSS-RNA), a thermodynamically stable, highly conserved stem loop that has been proposed as a therapeutic target. We describe the design, synthesis, and testing of a series of *N*-methyl peptides able to bind the HIV-1 FSS RNA stem loop with low nanomolar affinity and high selectivity. Surface plasmon resonance (SPR) data indicates increased affinity is a reflection of a substantially enhanced on rate. Compounds readily penetrate cell membranes and inhibit HIV infectivity in a pseudotyped virus assay. Viral infectivity inhibition correlates with compound-dependent changes in the ratios of Gag and Gag-Pol in virus particles. As the first compounds with both single digit nanomolar affinities for the FSS RNA and an ability to inhibit HIV in cells, these studies support the use of *N*-methylation for enhancing the affinity, selectivity, and bioactivity of RNA-binding peptides.

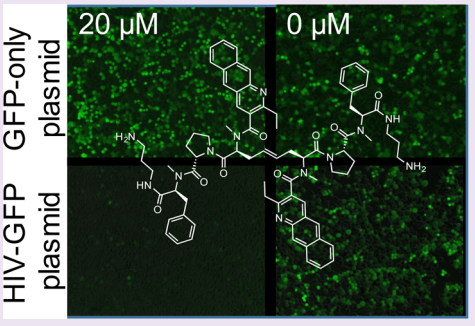

Human Immunodeficency Virus type 1 (HIV-1), like many retroviruses, encodes some of its proteins in an overlapping open reading frame (ORF) that does not contain its own ribosomal initiation site.[1] This overlapped ORF can only be translated by a programmed ribosomal frameshifting event. In HIV-1, the ORF encoding the polyprotein for viral enzymes (Pol) is in a −1 reading frame relative to that encoding the structural proteins (Gag). Pol is only translated with a frequency of 5−10% of Gag, reflecting how often frameshifting occurs.[2] Deviation from this narrow range causes defects in the virus' ability to infect new cells. This was robustly demonstrated by Shehu-Xhilaga et al. in 2001.[3] Using a reverse transcriptase activity assay as a marker for infectivity in 293T cells, viral fitness was found to degrade by approximately 100-fold as the Gag/Gag-Pol ratio changed from 20:1 to 20:21. These viral particles were also unable to correctly dimerize their genomic RNA, although recent work suggests that the frameshift site is not directly involved in packaging when the proper ratios of Gag/Gag-Pol are provided in trans.[4] Reduction in frameshift efficiency likewise interferes with viral replication.[5] Control of frameshifting in HIV-1 occurs via a frameshift stimulatory signal (FSS), a structured piece of the viral mRNA. Extensive analysis of this element, including NMR solution structures[6−8] and chemical probing using SHAPE,[9] suggests that a key structural feature of the HIV-1 FSS is a thermodynamically stable stemloop (Figure 1, boxed upper region). This is preceded by a heptameric, uridine-rich "slippery sequence," where the frameshift actually occurs, and other dynamically regulated regions of secondary structure.[9] The stemloop is highly conserved in HIV-1, with over 85% of all isolates containing the rare ACAA tetraloop motif,[6] and all subtypes of group M are predicted to fold into identical

Received: August 27, 2015
Accepted: October 23, 2015
Published: October 23, 2015

DOI: 10.1021/acschembio.5b00682
ACS Chem. Biol. 2016, 11, 88−94

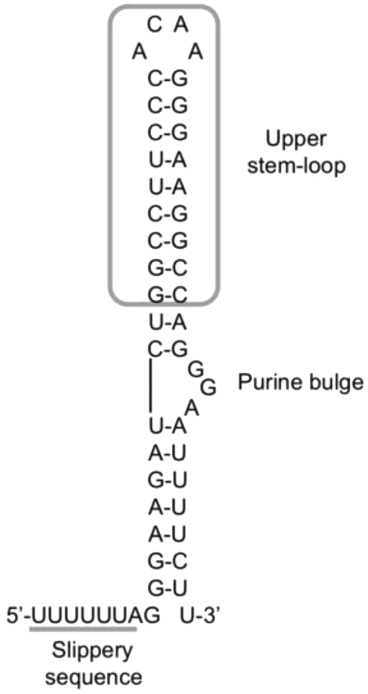

Figure 1. Secondary structure of isolated HIV frameshift-stimulating RNA and slippery sequence. In the context of the full HIV genome, SHAPE data suggest the lower stem and slippery sequence engage in other base-pairing interactions.[9] Boxed area: target sequence employed in this study.

secondary structures with a nearly 100% conservation of base pairs.[2]

Due to the virus' stringent control of the frequency of frameshifting, it has been suggested that small molecules able to bind the FSS-RNA and modulate this process could point the way to future HIV-1 therapeutics,[10,11] as well as serving as prototypes for small molecules able to interfere with recoding events in other viruses. Efforts to identify such compounds have been complicated by the general challenge posed by sequence-selective RNA recognition.[12−14] While a bisbenzamide,[15] doxorubicin,[16] and guanidinoneomycin[17] have been examined as FSS RNA binders, their relatively low affinities and lack of specificity have limited their applicability as probes or drug leads. Building on the discovery of an HIV-1 FSS RNA binder identified via Resin-Bound Dynamic Combinatorial Chemistry,[18] we recently reported the first synthetic compound able to bind the HIV-1 FSS RNA with a submicromolar dissociation constant and inhibit pseudotyped HIV infectivity.[19] Compound **1Z** was found to bind FSS RNA with a K_D of approximately 70 nM, was cell permeable, and strongly inhibited the infectivity of pseudotyped HIV in a dose-dependent manner. While successful, the selectivity of the **1Z**−FSS RNA binding interaction was modest (5:1 vs total yeast tRNA). In order to access compounds with enhanced anti-HIV activity and selectivity, we sought a simple modification that would be compatible with our synthetic scheme.

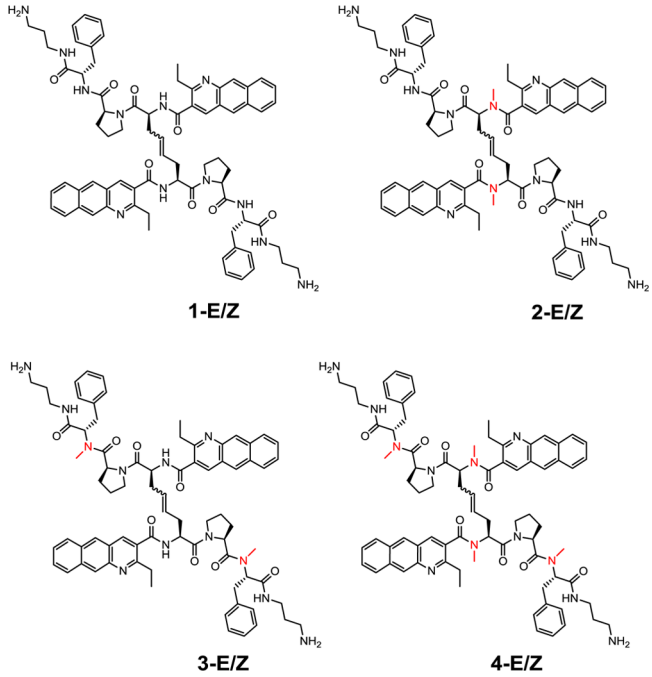

A strategy that has been used with success both in nature and by chemists for enhancing the affinity, selectivity, and activity of small peptides is *N*-methylation.[20,21] Nucleic acid binding natural products such as echinomycin,[22] the original inspiration for our resin-bound library design, incorporate *N*-methylation, and some of the highest affinity synthetic RNA binders known are *N*-methyl peptides.[20,21] *N*-Methylation has been shown to increase activity and selectivity of peptide based compounds that target CCK-A[23] and integrins.[24] It has also improved bioavailability in somatostatin analogs.[25] The mechanism for the improved selectivity and activity is thought to involve *N*-methylation-induced changes in conformational freedom;[26] an additional benefit is a reduction in susceptibility to protease-

Table 1. Fluorescence Titrations Confirm *N*-Methyl Analogs Have Higher Affinity and Selectivity for HIV-1 FSS RNA[a]

	sequence, K_D (nM)				
compound	FSS-RNA	FSS-DNA	yeast tRNA	FSS RNA: FSS DNA selectivity	FSS RNA: tRNA selectivity
1E	100 ± 30	230 ± 20	220 ± 30	2.3:1	2.2:1
1Z	66 ± 30	120 ± 20	330 ± 30	1.8:1	5:1
2E	2.7 ± 1.0	81 ± 30	120 ± 40	30:1	44:1
2Z	2.7 ± 0.7	65 ± 10	180 ± 20	24:1	67:1
3E	3.0 ± 0.1	79 ± 10	90 ± 10	26:1	30:1
3Z	1.1 ± 0.5	60 ± 8.0	67 ± 10	55:1	61:1
4E	5.0 ± 2.0	34 ± 10	91 ± 20	6.8:1	18:1

[a]Dissociation constants (K_D) are reported in nanomolarity. Titrations were carried out in 20 mM HEPES, 150 mM NaCl, and 5 mM $MgCl_2$. Each measurement was taken in triplicate to assure equilibrium was reached, and each titration was repeated twice. Data were fit to a single-site binding model. Error reported is the distance between values from complete titrations.

DOI: 10.1021/acschembio.5b00682
ACS Chem. Biol. 2016, 11, 88−94

mediated degradation.[27] As such, we hypothesized that introduction of *N*-methyl groups could bias the conformational ensemble of FSS-binding compounds favorably, resulting in higher affinity and enhanced frameshift-stimulating activity.

To test this hypothesis, a series of three different symmetrical methylation patterns were targeted. Combined with the potential to generate E and Z olefin isomers during synthesis, this would yield six new compounds. To that end, compounds **2**−**4E** and -**Z** were synthesized on a solid phase, via a scheme incorporating *N*-methylation methodology reported by Miller and Scanlan.[28] Five of the six targeted compounds were obtained in quantity; cross-metathesis to produce the tetra *N*-methyl compound did not yield a sufficient quantity of the Z isomer (**4Z**) to permit characterization.

RESULTS

***N*-Methylation Increases Binding Affinity and Selectivity for FSS-RNA.** The benzo[G]quinoline moiety of compounds **1**−**4** is fluorescent and quenches on binding DNA or RNA.[29] As such, fluorescence titration provides a simple, direct means for determining compound affinity. Dissociation constants (K_D) measured for compounds **1Z**−**4E** are reported in Table 1; titration curves are provided in the Supporting Information. In order to evaluate sequence selectivity, binding constants were also measured for each compound to total yeast tRNA (a standard selectivity measure)[30] and to a DNA sequence homologous to the FSS RNA. The concentration-independent melting profile of the latter suggests that it is also a hairpin or hairpin-like structure (Supporting Information). These results indicate that *N*-methylation enhanced compound affinity for the FSS-RNA relative to **1E** and **1Z** by as much as 100-fold and improved the selectivity relative to tRNA by 6- to 65-fold.

To confirm the high affinity binding and to determine if this resulted from changes in binding kinetics, compounds **3Z** and **4E** were further investigated by surface plasmon resonance. Compared to the previously reported compound **1Z**, *N*-methyl compounds **3Z** and **4E** both show an increase in k_a with little to no change in k_d (Table 2 and Supporting Information). This result is consistent with the hypothesis that *N*-methylation alters the conformational ensemble such that conformers close to the bound form are favored (faster k_a) but that the mode of binding is the same (no change in k_d). The small difference in K_D values measured between the two techniques is not unexpected, as SPR utilizes a surface immobilized RNA as opposed to the fully solution-phase fluorescence titration.

Table 2. SPR Confirms High Affinity Binding and Increased On Rate

compound	K_D (nM)	k_a (1/M*s)	k_d (1/s)
1Z[a]	71	$(2.2 \pm 0.8) \times 10^4$	$(1.4 \pm 0.1) \times 10^{-3}$
3Z[b]	6.7 ± 3.7	$(3.2 \pm 1.5) \times 10^5$	$(2.7 \pm 1.8) \times 10^{-3}$
4E[b]	13 ± 5.2	$(1.6 \pm 0.7) \times 10^5$	$(1.9 \pm 0.5) \times 10^{-3}$

[a]The values for compound **1Z** were previously reported.[19] [b]SPR was carried out in 150 mM NaCl and 10 mM HEPES. Injections were repeated twice for consistency. Curves were fit individually to a mass transfer model, and the error reported is standard deviation of all fits.

***N*-Methylation Increases Cell Permeability.** We used flow cytometry to assess the effect of *N*-methylation on the ability of HIV FSS-targeted compounds to cross cell membranes. Dose-dependent cell toxicity was first measured using a standard WST-1 proliferation assay[31] (Supporting Information S20) in HEK293T cells. These experiments established LD_{50} values for compounds **1Z**−**4E** in the range of 20−30 μM. For flow cytometry experiments, HEK293 cells were incubated with either 5 or 15 μM of each compound. Cells treated with *N*-methyl compounds show an increased amount of fluorescence at an equivalent concentration to unmethylated compound **1Z**, suggesting that *N*-methylation enhances the ability of HIV RNA-targeted compounds to cross the cell membrane (Figure 2).[32,33] The rank order of compound penetration (Figure 2) correlated strongly with differences in cLogP, with less-polar compounds displaying better permeability. Differences in permeability are also readily observable via fluorescence microscopy (Supporting Information).

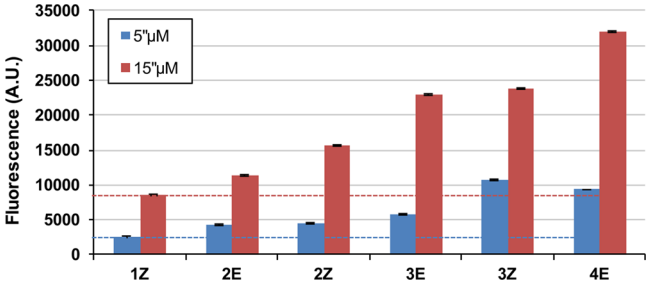

Figure 2. Cell permeability for HIV FSS-binding compounds, as measured by flow cytometry. HEK293T cells were incubated for 24 h in the presence of compound. Cells were then gated for negative propidium iodide and positive compound fluorescence. The mean intensity was calculated and plotted for each concentration (blue, 5 μM; red, 15 μM; dashed lines are provided for comparison to **1Z**). Error bars represent the rCV (robust coefficient of variation, or standard deviation divided by the median).

***N*-Methylation Increases Antiviral Potency.** To assess the effect of compounds **2E**−**4E** on viral fitness, an infectivity assay was performed with pseudotyped HIV.[34,23] HEK293T producer cells were transfected with a pro-viral plasmid for HIV in which the *nef* gene is replaced with green fluorescent protein and the *env* gene is deleted. A plasmid coding for VSV-G was cotransfected to allow for production of single cycle infectious virions. Producer cells were incubated with the compound for 24 h, after which the virions were harvested and normalized for viral load based on p24 ELISA. Equal loads of these viral particles were then incubated with TZM-bl reporter cells that express luciferase under long terminal repeat (LTR) promoter control when infected by HIV-1. All new compounds with the exception of **2E** showed significantly greater antiviral activity in this assay than our previously reported compound **1Z**, with compound **4E** exhibiting the most potent activity (Figure 3). Data shown in the figure are a composite from two experiments; additional data may be found in the Supporting Information. While factors governing activity in this assay are complex, the enhanced potency of the *N*-methyl compounds likely is a function of both their enhanced affinity for the FSS RNA and improved cell permeability. To ensure reproducibility of the observed biological effect, infectivity inhibition assays were repeated for select compounds in a second laboratory (Supporting Information S27).

***N*-Methyl Compounds Increase Gag-Pol Levels in Virions.** We next assayed viral protein production as a function of added compounds **2**−**4** to determine if inhibition of

DOI: 10.1021/acschembio.5b00682
ACS Chem. Biol. 2016, 11, 88−94

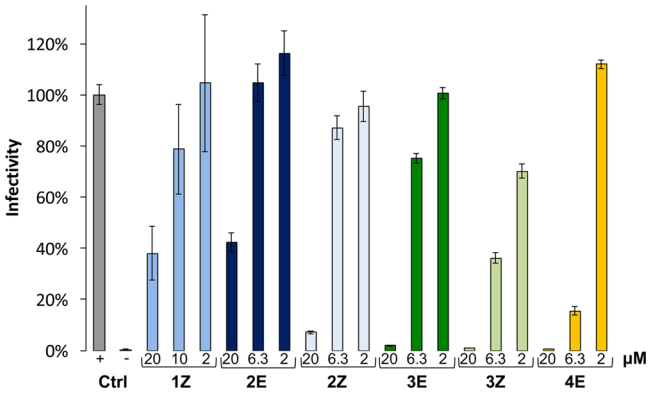

Figure 3. *N*-methyl compounds demonstrate enhanced antiviral potency. HEK293T producer cells were transfected for 4 h with pro-viral and VSV-G plasmids to produce single cycle infectious particles. The producer cells were then incubated for 24 h in the presence of compound, in triplicate for each condition. Virions were harvested, normalized, then incubated with TZM-bl reporter cells. Luciferase production from the reporter cells was measured and normalized to values obtained from control cells. Error bars indicate standard deviation.

infectivity correlated with increased amounts of frameshift products. Viral particles were collected and their proteins analyzed by SDS-PAGE and Western blotting. The primary antibody reacted with the blots recognized p160, the full length Gag-Pol polyprotein that is only made if the −1 frameshift occurs, as well as with p55 and p24, two forms of Gag that are made with or without frameshifting (Figure 4). The ratio of p160 to p24+p55 was determined as a semiquantitative measure of frameshifting. We observed that this ratio increases in a dose-dependent manner and correlated strongly with the ability of individual compounds to inhibit the infectivity of pseudotyped virions. As these ratios could be affected by packaging bias, we also examined Gag/Gag-Pol ratios directly in the cell lysates of producer cells (Supporting Information). We observed similar trends to those obtained from virus particles. In tandem, these results are consistent with a direct concentration-dependent enhancement of FSS RNA-binding compounds on frameshifting.

To control for the possibility that FSS-binding compounds might also interact with viral protease, results were compared with an analogous assay including the FDA-approved protease inhibitor, indinavir. We observed that indinavir increased the amount of p55 visible on the blot, while dramatically decreasing the amount of p24. No buildup of p160 was observed. These results strongly contrast with those observed for compounds **2**−**4**. We further confirmed that compound activity is independent of HIV protease via a commercial protease inhibition assay (Supporting Information Figure S-9). The compounds do not show any significant protease inhibition up to 100 μM.

DISCUSSION

While several authors have hypothesized that compound-dependent frameshift enhancement could serve as an effective means of limiting viral infectivity,[10,11,15,16,37] the lack of high affinity, sequence-selective frameshift RNA-binding compounds has made testing this hypothesis a challenge. Compounds we reported previously reduced the infectivity of pseudotyped virions and enhanced frameshifting, but their modest selectivity for the FSS RNA suggested that the antiviral activity could be due to a variety of mechanisms. Here, we find that antiviral activity and changes in Gag/Gag-Pol in produced pseudotyped virus particles strongly correlates with affinity for the HIV-1 FSS RNA, as well as cell permeability.

The enhanced on rates observed by SPR for **3Z** and **4E** relative to the non-*N*-methylated compound **1Z** are intriguing. Very little is known about the relationship of binding kinetics and selectivity for RNA-targeted molecules. This is in contrast to proteins, for which a consensus is emerging that selectivity and efficacy are direct functions of the off rate (frequently described as the "residence time").[35,36] For RNA, and nucleic acids generally, such a broad generalization is probably not possible, as there are clearly nonselective binders (for example, many intercalators) with slow off-rates. Here, we observe an increase in affinity and selectivity for compounds with enhanced on-rates, but comparable off-rates. We hypothesize that, as with other *N*-methyl peptides, the enhanced on-rates are the result of differences in the ground-state conformational ensemble in which the proportion of binding-favorable conformers are enhanced. Structural studies designed to test that hypotheses are in progress.

To date, these compounds show the highest affinity for the FSS-RNA and are the only class of molecules that alters the products of frameshifting and inhibits viral infectivity.[37] Tetramethylated compound **4E** has the greatest increase in

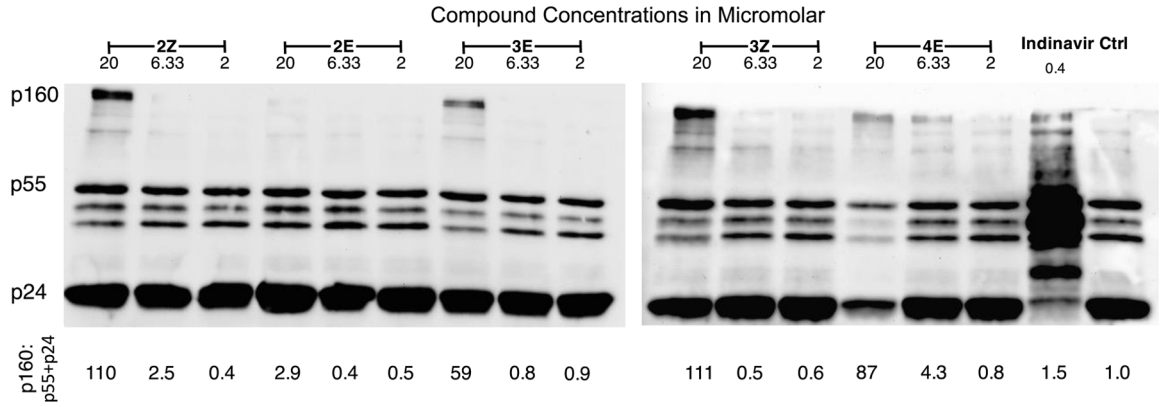

Figure 4. Virions collected and their proteins harvested and run on an SDS-PAGE gel. The transferred blot was then probed with an anti-p24 antibody, which will mark p24, as well as its precursor proteins p55 and p160. The ratio of p160 to p24+p55 was calculated by scanning densitometry (UVP VisionWorks software). The 20 μM lane for **4E** was loaded with half as much protein due to a limiting quantity of virions.

DOI: 10.1021/acschembio.5b00682
ACS Chem. Biol. 2016, 11, 88−94

hydrophobicity relative to **1** and also was the most cell-permeable. Further, **4E** showed the greatest ability to inhibit the production of infectious virions. Interestingly, **4E** also affected not only the ability to make infectious virions but also severely limited the intracellular replication of the virus, as can be visualized via GFP production from the proviral plasmid in HEK 293T producer cells (Figure 5). Thus, both the

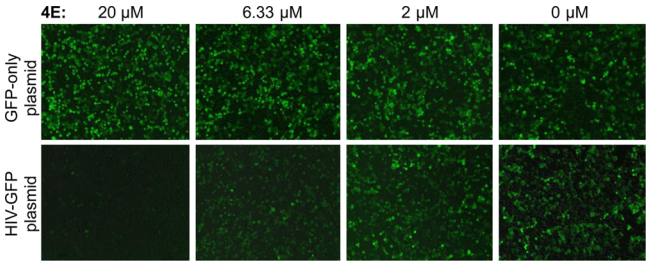

Figure 5. Treatment with compound **4E** interferes with replication of an HIV-GFP plasmid in producer cells.

compound interferes with production of virus particles and the particles produced are less infective. While the availability of the compound increases with hydrophobicity, and appears to be the major limiting factor for antiviral effects, the discrepancy between compound **2E** and **3E** indicates that the increase in hydrophobicity is not the only governing factor for cell penetration. Based on the various patterns of *N*-methylation, it is not unreasonable to hypothesize that the differences are due to changes in the conformational ensembles of these molecules. More broadly, these results support the general hypothesis that synthetic molecules can have useful biological effects, when targeted to RNAs believed to have regulatory roles in protein recoding. Given the breadth of critical RNA-regulated frameshifting events discovered in viruses,[38−40] bacteria,[41,42] and even humans,[43,44] further exploration of this strategy in the context of understanding basic biology and the development of therapeutics is warranted.

MATERIALS AND METHODS

FSS-RNA and DNA were purchased from Integrated DNA Technologies and assessed for purity and structure using thermal melting protocols. Yeast tRNA was purchased from Sigma-Aldrich and used without further purification. Amino acids were purchased from P3Bio and used as received.

Fluorescence Titration. Fluorescence titrations were carried out in 20 mM HEPES, 150 mM NaCl, and 5 mM $MgCl_2$, using a Horiba FluoroMax 4 fluorometer. All titrations started at a volume of 500 μL with the compound at 20−500 nM. The concentration was chosen based on a preliminary titration using 1 μM compound to get a first approximation of the binding affinity and then lowered to more accurately measure the affinity. RNA was then titrated in from a high concentration stock (0.5−10 μM for HIV-1 FSS RNA; 10 μM for HIV-1 FSS DNA and tRNA) in 1−10 μL increments. After RNA was added, the solution was thoroughly mixed in the cuvette via pipetting and allowed to stand for 10 min to reach equilibrium. Each measurement was taken three times with a 1 min waiting period between scans to confirm equilibrium was reached. Intensities were corrected for dilution. All titrations were completed twice.

Surface Plasmon Resonance. SPR was conducted using a Biacore X (Biacore, Inc.). Compounds were injected at a flow rate of 30 μL/min in 10 mM HEPES and 150 mM NaCl for 2 min. Flow was then maintained for at least 1 h to allow for dissociation. Each injection was repeated twice for consistency. Each trace was fit individually to a mass transfer model.

Cell Toxicity. HEK293T cells were plated at 1×10^4 cells/well in a 96 well plate in DMEM with 10% fetal bovine serum and 1% anti−anti (penicillin-streptomycin + fungizone) at 37 °C. After cells were allowed to adhere for 6 h, they were then incubated with the compound for 24 h in triplicate. A total of 10 μL of WST-1 premix (Clontech) was added and incubated for 1 h followed by measurement using a PerkinElmer EnSpire plate reader.

Flow Cytometry. HEK293T cells were grown in DMEM with 10% fetal bovine serum and 1% penicillin-streptomycin at 37 °C to 80% confluency in a 12-well plate and treated with the compound for 24 h. Cells were trypsinized, pelleted, and washed twice with DPBS (Gibco). Cells were then resuspended in 300 μL ice cold DPBS and incubated with 5 μL of propidium iodide to stain dead cells. A total of 10 000 events were collected using a BD LSR-II flow cytometer.

HIV-1 Infectivity. The antiviral activity of all RNA-targeted compounds was measured by single-round infectivity assay with pseudotyped HIV-1 using HEK293T producer cells. The HIV-1 proviral vector (pDHIV3-GFP) includes all HIV-1 NL4−3 genes except *nef* (replaced with GFP) and *env*, thus preserving *gag* and *pol*, and the frameshift required for production of the Gag-Pol polyprotein. A single-round infectivity assay was conducted by transient transfection of the viral vector with VSV-G coat protein vector at a ratio of 1:0.5 using Fugene HD (Promega). The virus producer cells were dosed with compounds 4 h after transfection, and viral particles were harvested from the media 24 h after transfecting by filtering through a 0.45-μm syringe filter. Viral load was normalized with a p24 ELISA (PerkinElmer). The infections were performed using TZM-bl reporter cells containing stably integrated firefly luciferase, the expression of which is driven by the HIV-LTR promoter. Therefore, luciferase is expressed upon successful HIV infection. Triplicate infections in 96-well plates at 10 000 cells/well with 500 pg p24/well proceeded for 48 h before the addition of SteadyGlo reagent (Promega) to each well for 30 min. Luminescence was measured as a quantitative metric for changes in viral infectivity in the presence of a compound.

Protease Inhibition. The protease inhibition kit was purchased from Protein One and used as instructed. HIV-1 Protease was incubated at RT with no compound, a protease inhibitor, or compound for 90 min in the presence of the peptide FRET substrate. Each condition was made in triplicate in a 96 well plate, and the fluorescence was measured using 490 nm excitation and 530 nm emission using a PerkinElmer EnSPire plate reader.

ASSOCIATED CONTENT

Supporting Information

The Supporting Information is available free of charge on the ACS Publications website at DOI: 10.1021/acschembio.5b00682.

Synthesis of compounds, compound characterization, fluorescence titrations, characterization of nucleic acid (DNA and RNA) sequences, surface plasmon resonance measurements, cell toxicity measurements, protease inhibition assay, flow cytometry data, fluorescence microscopy, additional Western blotting experiments, and replicate viral infectivity assay data (PDF)

AUTHOR INFORMATION

Corresponding Author

*E-mail: Benjamin_miller@urmc.rochester.edu.

Notes

The authors declare no competing financial interest.

ACKNOWLEDGMENTS

We thank Dr. Glynis Scott (University of Rochester) for the donation of HEK293 cells and the Flow Core at the University of Rochester for assisting with flow cytometry experiments. We thank SUNY Geneseo for use of their NMR spectrometer,

DOI: 10.1021/acschembio.5b00682
ACS Chem. Biol. 2016, 11, 88−94

supported by a Congressionally directed grant from the U.S. Department of Energy (grant no. DE-SC0005129). This research was supported by the National Institutes of Health through research grants GM100788 (to B.L.M.) and GM072447 (to S.E.B) and Institutional Ruth L. Kirschstein National Research Service Awards GM068411 and AI049815 (T.A.H.)

REFERENCES

(1) Brierley, I. (1995) Ribosomal frameshifting viral RNAs. *J. Gen. Virol. 76*, 1885−1892.
(2) Baril, M., Dulude, D., and Gendron, K. (2003) Efficency of a programmed −1 ribosomal frameshift in the different subtypes of the HIV-1 group M. *RNA 9*, 1246−1253.
(3) Shehu-Xhilaga, M., Crowe, S., and Johnson, M. (2001) Maintenance of the Gag/Gag-Pol ratio is important for HIV-1 RNA Dimerization and Viral Infectivity. *J. Virol. 75*, 1834−1831.
(4) Nikolaitchik, O. A., and Hu, W.-S. (2014) Deciphering the role of the Gag-Pol ribosomal frameshift signal in HIV-1 RNA genome packaging. *J. Virol. 88*, 4040−4046.
(5) Dulude, D., Berchiche, Y. A., Gendron, K., Brakier-Gingras, L., and Heveker, N. (2006) Decreasing the frameshift efficiency translates into an equivalent reduction of the replication of the human immunodeficiency virus type 1. *Virology 345*, 127−136.
(6) Staple, D., and Butcher, S. (2003) Solution Structure of the HIV-1 frameshfit inducing stem-loop RNA. *Nucleic Acids Res. 31*, 4326−4331.
(7) Staple, D. W., and Butcher, S. E. (2005) Solution structure and thermodynamic investigation of the HIV-1 frameshift inducing element. *J. Mol. Biol. 349*, 1011−1023.
(8) Gaudin, C., Mazauric, M.-H., Traïkia, M., Guittet, E., Yoshizawa, S., and Fourmy, D. (2005) Structure of the RNA signal essential for translational frameshifting in HIV-1. *J. Mol. Biol. 349*, 1024−1035.
(9) Low, J. T., Garcia-Mirana, P., Mouzakis, K. D., Groelick, R. J., Butcher, S. E., and Weeks, K. M. (2014) Structure and dynamics of the HIV-1 frameshift element RNA. *Biochemistry 53*, 4282−4292.
(10) Biswas, P., Jiang, X., Pacchia, A. L., Dougherty, J. P., and Peltz, S. W. (2004) The human immunodeficiency virus type 1 ribosomal frameshifting site is an invariant sequence determinant and an important target for antiviral therapy. *J. Virol. 78*, 2082−2087.
(11) Gareiss, P. C., and Miller, B. L. (2009) Ribosomal frameshifting: An emerging drug target for HIV. *Curr. Opin. Invest. Drugs 10*, 121−128.
(12) Thomas, J., and Hergenrother, P. (2008) Targeting RNA with Small molecules. *Chem. Rev. 108*, 1171−1224.
(13) Guan, L., and Disney, M. (2012) Recent Advances in developing small molecules targeting RNA. *ACS Chem. Biol. 7*, 73−86.
(14) Blakeley, B. D., DePorter, S. M., Mohan, U., Burai, R., Tolbert, B. S., and McNaughton, B. R. (2012) Methods for identifying and characterizing interactions involving RNA. *Tetrahedron 68*, 8837−8855.
(15) Hung, M., Patel, P., Davis, S., and Green, S. R. (1998) Importance of ribosomal frameshifting for human immunodeficiency virus type 1 particle assembly and replication. *J. Virol. 72*, 4819−4824.
(16) Marcheschi, R., Tonelli, M., Kumar, A., and Butcher, S. (2011) Structure of the HIV-1 frameshift site RNA bound to a small molecule inhibitor of viral replication. *ACS Chem. Biol. 6*, 857−864.
(17) Staple, D., Venditti, V., Niccolai, N., Elson-Schwab, L., Tor, Y., and Butcher, S. (2008) Guanidinoneomycin B recognition of an HIV-1 RNA helix. *ChemBioChem 9*, 93−102.
(18) McNaughton, B., Gareiss, P., and Miller, B. (2007) Identification of a selective small-molecule ligand for HIV-1 frameshift-inducing stem-loop RNA from an 11,325 member resin bound dynamic combinatorial library. *J. Am. Chem. Soc. 129*, 11306−11307.
(19) Ofori, L., Hilimire, T., Bennett, R., Brown, N., Smith, H., and Miller, B. (2014) High-affinity recognition of HIV-1 frameshift-stimulating RNA alters frameshifting in vitro and interferes with HIV-1 infectivity. *J. Med. Chem. 57*, 723−732.
(20) Athanassiou, Z., Patora, K., Dias, R. L., Moehle, K., Robinson, J. A., and Varani, G. (2007) Structure-guided peptidomimetic design leads to nanomlar β-hairpin inhibitors of the tat-TAR interaction of bovine immunodeficiency virus. *Biochemistry 46*, 741−751.
(21) Moehle, K., Athanassiou, Z., Patora, K., Davidson, K., Varani, G., and Robinson, J. A. (2007) Design of β-hairpin peptidomimetics that inhibit binding of α-helical HIV-1 Rev protein to the Rev Response Element RNA. *Angew. Chem., Int. Ed. 46*, 9101−9104.
(22) Socha, A., LaPlante, K., Russell, D., and Rowley, D. (2009) Structure − activity studies of echinomycin antibiotics against drug-resistant and biofilm-forming *Staphyloccus aureus* and *Enterococcus faecalis*. *Bioorg. Med. Chem. Lett. 19*, 1504−1507.
(23) Holladay, M., Kopecka, H., Miller, T., Bednarz, L., Nikkel, A., Bianchi, B., Witte, D., Shiosaki, K., Lin, C., Asin, K., and Nadzan, A. (1994) Tetrapeptide CCK-A agonists: effect of backbone N-methylations on *in Vitro* and *in Vivo* CCK activity. *J. Med. Chem. 37*, 630−635.
(24) Chatterjee, J., Ovadia, O., Zahn, G., Marinelli, L., Hoffman, A., Gilon, C., and Kessler, H. (2007) Multiple N-methylation by a designed approach enhances receptor selectivity. *J. Med. Chem. 50*, 5878−5881.
(25) Biron, E., Chatterjee, J., Ovadia, O., Langenegger, D., Brueggen, J., Hoyer, D., Schmid, H. A., Jelinek, R., Gilon, C., Hoffman, A., and Kessler, H. (2008) Improving oral bioavailability of peptides by multiple N-methlyation: somatostatin analgoues. *Angew. Chem., Int. Ed. 47*, 2595−2599.
(26) Chatterjee, J., Mierke, D., and Kessler, H. (2008) Conformational preference and potential templates of N-methylated cyclic pentaalanine peptides. *Chem. - Eur. J. 14*, 1508−1517.
(27) Chatterjee, J., Rechenmacher, F., and Kessler, H. (2013) N-methylation of peptides and proteins: an important method for modulating biological functions. *Angew. Chem., Int. Ed. 52*, 254−269.
(28) Miller, S., and Scanlan, T. (1997) Site-selective N-methylation of peptides on solid support. *J. Am. Chem. Soc. 119*, 2301−2302.
(29) Ofori, L. O., Hoskins, J., Nakamori, M., Thornton, C. A., and Miller, B. L. (2012) From dynamic combinatorial 'hit' to lead: *in vitro* and *in vivo* activity of compounds targeting the pathogenic RNAs that cause myotonic dystrophy. *Nucleic Acids Res. 40*, 6380−6390.
(30) Luedtke, N., Liu, Q., and Tor, Y. (2003) RNA-ligand interactions: affinity and specificity of aminoglycoside dimers and acridine conjugates to the HIV-1 Rev Response Element. *Biochemistry 42*, 11391−11403.
(31) Buttke, T., McCubrey, J., and Owen, T. (1993) Use of an aqeous soluble tetrazolium/formazan assay to measure viability and proliferation of lymphokine-dependent cell lines. *J. Immunol. Methods 157*, 233−240.
(32) Bautista, A., Appelbaum, J., Craig, C., Michel, J., and Schepartz, A. (2010) Bridged β^3-peptide inhibitors of p53-hDM2 complexation-correlation between affinity and cell permeability. *J. Am. Chem. Soc. 132*, 2904−2906.
(33) Bernal, F., Tyler, A., Korsmeye, S., Walensky, L., and Verdine, G. (2007) Reactivation of the p53 tumor suppressor pathway by a stapled p53 peptide. *J. Am. Chem. Soc. 129*, 2456−2457.
(34) Platt, E. J. E., Wehrly, K. K., Kuhmann, S. E. S., Chesebro, B. B., and Kabat, D. D. (1998) Effects of CCR5 and CD4 cell surface concentrations on infections by macrophagetropic isolates of human immunodeficiency virus type. *J. Virol. 72*, 2855−2864.
(35) Copeland, R. A., Pompliano, D. L., and Meek, T. D. (2006) Drug-target residence time and its implications for lead optimization. *Nat. Rev. Drug Discovery 5*, 730−739.
(36) Bradshaw, J. M., McFarland, J. M., Paavilainen, V. O., Bisconte, A., Tam, D., Phan, V. T., Romanov, S., Finkle, D., Shu, J., Patel, V., Ton, T., Li, X., Loughhead, D. G., Nunn, P. A., Karr, D. E., Gerritsen, M. E., Funk, J. O., Owens, T. D., Verner, E., Brameld, K. A., Hill, R. J., Goldstein, D. M., and Taunton, J. (2015) Prolonged and tunable residence time using reversible covalent kinase inhibitors. *Nat. Chem. Biol. 11*, 525−531.

DOI: 10.1021/acschembio.5b00682
ACS Chem. Biol. 2016, 11, 88−94

(37) Brakier-Gingras, L., Charbonneau, J., and Butcher, S. (2012) Targeting frameshifting in the human immunodeficiency virus. *Expert Opin. Ther. Targets 16*, 249−258.
(38) Plant, E. P., Pérez-Alvarado, G. C., Jacobs, J. L., Mukhopadhyay, B., Hennig, M., and Dinman, J. D. (2005) A three-stemmed mRNA pseudoknot in the SARS coronavirus frameshift signal. *PLoS Biol. 3* (e172), 1012−1023.
(39) Falk, H., Mador, N., Udi, R., Panet, A., and Honigman, A. (1993) Two cis-acting signals control ribosomal frameshift between human T-cell leukemia virus type II gag and pro genes. *J. Virol. 67*, 6273−6277.
(40) Dos Ramos, F., Carrasco, M., Doyle, T., and Brierley, I. (2004) Programmed −1 ribosomal frameshifting in the SARS coronavirus. *Biochem. Soc. Trans. 32*, 1081−1083.
(41) Larsen, B., Gesteland, R. F., and Atkins, J. F. (1997) Structural probing and mutagenic analysis of the stem-loop required for Escherichia coli dnaX ribosomal frameshifting: programmed efficiency of 50%. *J. Mol. Biol. 271*, 47−60.
(42) Antonov, I., Coakley, A., Atkins, J. F., Baranov, P. V., and Borodovsky, M. (2013) Identification of the nature of reading frame transitions observed in prokaryotic genomes. *Nucleic Acids Res. 41*, 6514−6530.
(43) Below, A. T., Meskauskas, A., Musalgaonkar, S., Advani, V. M., Solima, S. O., Kasprzak, W. K., Shapiro, B. A., and Dinman, J. D. (2014) Ribosomal frameshifting in the CCR5 mRNA is regulated by miRNAs and the NMD pathway. *Nature 512*, 265−269.
(44) Belew, A. T., and Dinman, J. D. (2015) Cell cycle control (and more) by programmed −1 ribosomal frameshifting: implications for disease and therapeutics. *Cell Cycle 14*, 172−178.

DOI: 10.1021/acschembio.5b00682
ACS Chem. Biol. 2016, 11, 88−94